AJNR

MR of the inner ear in patients with Cogan syndrome.

J W Casselman, M H Majoor and F W Albers

AJNR Am J Neuroradiol 1994, 15 (1) 131-138
http://www.ajnr.org/content/15/1/131

MR of the Inner Ear in Patients with Cogan Syndrome

Jan W. Casselman, M. H. J. M. Majoor, and Frans W. Albers

PURPOSE: To determine whether the bony and soft-tissue obliterations of the intralabyrinthine fluid spaces reported in pathologic studies of patients with Cogan syndrome can be detected with MR or CT. **METHODS:** The inner ears of six patients with Cogan syndrome were studied. High-resolution CT was performed in five patients; all six patients were studied with MR, including T1-weighted spin-echo images with and without gadolinium administration, T2-weighted spin-echo images, and three-dimensional Fourier transform constructive interference in steady state images. **RESULTS:** In two patients, small calcified obliterations were detected on CT but the three-dimensional Fourier transform constructive interference in steady state images revealed more extensive soft-tissue obliteration in five of the six patients. High signal inside the membranous labyrinth on precontrast T1-weighted images and contrast enhancement inside the membranous labyrinth on the postcontrast T1-weighted images were seen in one patient. **CONCLUSIONS:** The study showed that calcific obliteration and soft-tissue obliteration of the intralabyrinthine fluid spaces in patients with Cogan syndrome can be demonstrated radiologically and that soft-tissue obliteration is more frequent than calcified obliteration. MR detected the intralabyrinthine disease far more frequently than did CT. The three-dimensional Fourier transform constructive interference in steady state sequence proved to be the most sensitive MR sequence. Hyperintensity inside the membranous labyrinth on the precontrast T1-weighted images and enhancement on the contrast-enhanced T1 images were less frequent and probably represent leakage through the abnormal labyrinthine membrane from active disease.

Index terms: Ear, abnormalities and anomalies; Ear, magnetic resonance; Temporal bone, abnormalities and anomalies; Temporal bone, magnetic resonance; Nervous system, diseases; Magnetic resonance, technique

AJNR Am J Neuroradiol 15:131–138, Jan 1994

Cogan syndrome is a rare syndrome affecting young adults. The patients present with nonsyphilitic interstitial keratitis and audiovestibular dysfunction (1–3). Associated cardiac and diffuse vascular lesions are often detected. The prognosis for vision is good, although permanent deafness occurs in most instances. Pathologic studies have mentioned obliteration of the endo- and perilymphatic fluid spaces in these patients caused by acidophilic coagulum, cellular debris, connective tissue, hypertrophy of the stria vascularis, and even pathologic bone formation.

We studied six patients with Cogan syndrome to determine whether these bony and/or soft-tissue obliterations of the intralabyrinthine fluid spaces (IFS) reported in pathologic studies could be detected with computed tomography (CT) or magnetic resonance (MR). CT was used to detect calcifications in the IFS and a three-dimensional Fourier transform (3DFT) constructive interference in steady state (CISS) MR sequence was used to look for soft-tissue obliteration of the IFS.

This 3DFT MR technique has already been proved to be very sensitive for the detection of intralabyrinthine soft-tissue obliterations (4, 5). With the use of both CT and MR, differentiation between bony and soft-tissue obliteration is possible and the frequency of both types of obliteration can be evaluated.

Received September 10, 1992; accepted pending revision November 15; revision received January 20, 1993.

From the Department of Radiology, A.Z. St. Jan Hospital, Brugge, Belgium (J.W.C.); the Department of Otorhinolaryngology, University Hospital, Utrecht, the Netherlands (M.H.J.M.M.); and the Department of Otorhinolaryngology, University Hospital, Gent, Belgium (F.W.A.).

Presented at the 30th Annual Meeting of the ASNR, St. Louis, Missouri, May 31 to June 5, 1992.

[1] Address reprint requests to: J.W. Casselman, Department of Radiology, A.Z. St. Jan Brugge, Ruddershove 10, B-8000 Brugge, Belgium.

AJNR 15:131–138, Jan 1994 0195-6108/94/1501-0131

Finally, T1-weighted images with and without intravenous gadolinium administration were used to detect abnormal contrast enhancement in the membranous labyrinth (ML).

Subjects and Methods

Six patients with Cogan syndrome (5 men, 1 woman; average age, 25 years) underwent radiologic examination of the temporal bones. The diagnosis of Cogan syndrome was made when the clinical symptoms were in agreement with the diagnostic criteria formulated by Cogan (6). Therefore, only patients with a typical nonulcerative stromal keratitis in conjunction with audiovestibular symptoms in the absence of congenital syphilis were selected for the study.

Five patients underwent a coronal and axial high-resolution CT scan (9800 Hilight, General Electric, Milwaukee, Wis). Section thickness was 1.5 mm and sections were made every 1 mm. We looked for calcific obliteration of the IFS on these CT images.

All patients were also studied with MR on a 1.0 tesla superconductive active shielded magnet (Magnetom SP 42, Siemens, Erlangen). They were studied with 3-mm contiguous two-dimensional spin-echo T1-weighted images without and with intravenous gadolinium administration 500/15/4 (repetition time/echo time/excitations) and 4-mm-thick axial two-dimensional spin-echo T2-weighted images 2500/15, 90/1 with a 0.8-mm gap.

Finally, 1-mm thick contiguous axial 3DFT CISS images were acquired in all patients. The basic principles and description of the 3DFT CISS sequence scheme have been reported (4, 5, 7, 8). Fast imaging with steady precession (FISP) and contrast-enhanced fast-acquisition steady-state sequences basically rely on the steady state of both longitudinal and transversal magnetization (9, 10). This steady state is established by excitation of the spin system with radio frequency pulses at a short repetition time $\ll$ T2. The development of this state is achieved using a short equilibration time of about 1 second before starting the data acquisition itself. As is well known from flow imaging, moving spins will accumulate additional phase shifts when moving along field gradients. If the motion is not constant in time, transverse magnetization will experience random phase shifts and the magnetization may cancel completely, thus completely avoiding a steady state of the transverse magnetization. Therefore, moving cerebrospinal fluid does not produce any signal when standard FISP or contrast-enhanced fast-acquisition steady-state sequences are used. Even for very slow flow, the cerebrospinal fluid signal may disappear because these flow-induced phase shifts will accumulate over many repetition time intervals, thus creating a large amount of phase shifts in the magnetization.

Flow-compensation techniques have to be used to ensure that spins, independent of their actual velocity, are being refocused. The flow compensation must be applied to each gradient over each repetition time cycle, unlike standard flow-compensation sequences (eg, motion-refocusing angiography sequences), in which the flow compensation is applied to the echo. A steady-state flow-compensated three-dimensional FISP sequence is shown in Figure 1. All three gradients are balanced, indicating that the average value of each gradient is zero. In this case, spins moving at a constant velocity will have the same phase

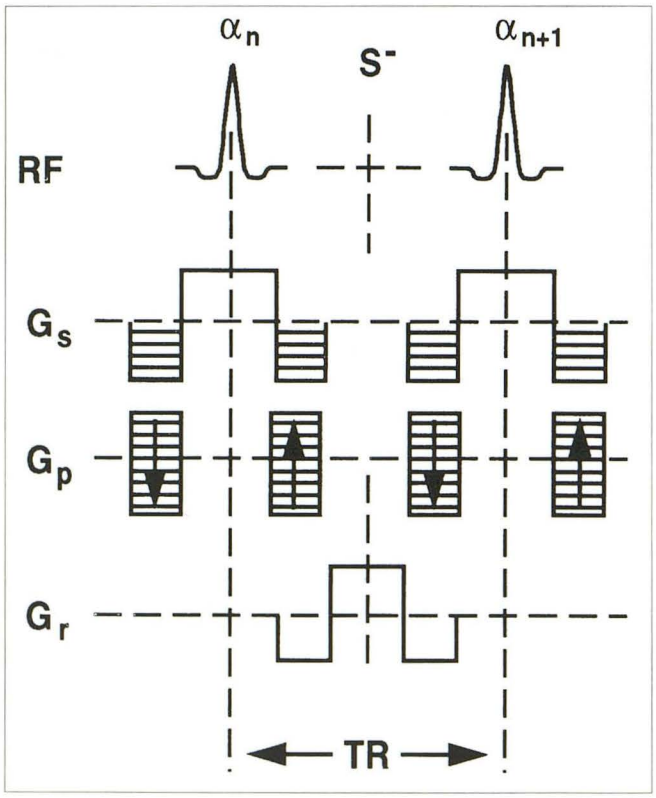

Fig. 1. True three-dimensional FISP sequence. The three gradients are balanced indicating that the average value of each gradient in the section selection (Gs), phase encoding (Gp) and frequency encoding (Gr) direction is zero. This true FISP sequence is repeated twice when the CISS sequence scheme is used, once with nonalternating radio frequency ($\alpha n = \alpha n + 1 = \alpha{+}{+}$) and once with alternating radio frequency ($\alpha n = \alpha n + 1 = \alpha + -$).

after the application of the gradient pulses as they had before (7). Running a sequence as shown in Figure 1 will produce an image that shows bands of low signal intensity. The occurrence of these bands is not a result of any system imperfection but is related to basic physical effects. These dark bands are caused by very small magnetic-field inhomogenities and local field distortions attributable to susceptibility changes that are normally produced by the patient. These inhomogenities cause corresponding frequency offsets. If the frequency at a given location is such that the phase angle accumulation over one repetition time period corresponds to π, or odd integers thereof, the magnetization cancels, and a dark point appears in the image. At another location, the frequency offset might be larger (eg, 2 π or a multiple thereof), and the magnetization will interfere constructively, resulting in a high signal intensity at this particular point.

The solution to this inherent problem is to acquire two data sets successively with a "true FISP" (9) sequence of alternating (+−) and nonalternating (++) radio frequency pulses. The position of the dark bands is shifted in the second data set to the position of high intensity of the first data set. A simple mathematical postprocessing operation (maximum intensity projection [11]) takes the information of each pair of images of the two three-dimensional data sets and produces an image with a homogeneous intensity distribution over the whole image and very good contrast between the high-signal intralabyrinthine fluid and the low signal of the surrounding bony labyrinth. Moreover, the 1-mm-thin contiguous sections allow detailed evaluation of the ML and IFS and can minimize partial volume artifacts (4, 5).

Each data set covers a volume of 32 mm for application in the inner ear. This slab is divided into 32 partitions, resulting in an effective section thickness of 1 mm. The measurement parameters are: 20/8, matrix size 256 × 256, field of view 176 mm, and flip angle 50°. The result is a total acquisition time of 2 times 2.46 minutes and an inplane resolution of each of the three-dimensional partitions of 0.69 × 0.69 mm.

A targeted maximum intensity projection on the CISS data set also allows three-dimensional reconstructed imaging of the inner ear (14). The use of a field of view of 176 mm also allows examination of both inner ears when the head coil is used.

On all MR images we looked for obliteration of the IFS inside the three semicircular canals, the common crus, the vestibule, and the basal and second/apical turn of the cochlea. The use of both CT and MR made differentiation between "bony" and "fibrous" obliteration possible. Bony or calcified obliteration can be seen as calcifications or regions of high density inside the IFS on CT images, and on MR images at the same site obliteration (signal loss) of the IFS is seen. Fibrous obliteration is present when no calcific obliteration is seen on CT and loss of high signal of the intralabyrinthine fluid is found on the MR images. Finally, we also checked whether gadolinium enhancement inside the ML occurred, indicating leakage of gadolinium through the abnormal labyrinthine membrane.

Results

All patients had bilateral sensorineural hearing loss with tinnitus and vertigo. An interstitial keratitis was seen in each patient. All six patients experienced a period of general illness with fatigue. Two patients also had arthralgia. Two men had testicular pain. One patient complained of myalgia. One had multiple aneurysms of the major abdominal and thoracic arteries. An increased erythrocyte sedimentation rate and leucocytosis were found in all patients. All serologic tests for syphilis were negative.

Obliteration of the IFS was seen in 5 of the 6 patients on the 3DFT CISS images, and calcification inside the IFS was detected in 2 patients (Table 1). In these 2 patients calcifications were found in the basal turn of the cochlea near the round window in 3 temporal bones and bony narrowing of the lateral semicircular canal was seen in one inner ear. In one patient high signal intensity was present inside the cochlea and vestibule on the unenhanced T1-weighted images

TABLE 1: Sensitivity of CT and different MR sequences in the detection of obliteration of the intralabyrinthine fluid spaces in 6 patients with Cogan syndrome

Case	Sex	CT	T1	T2	CISS	T1-Gadolinium
1	Male	−	−	−	−	−
2	Female	−	+	−	+	*
3	Male	NA[a]	−	−	+	−
4	Male	+	−	−	+	−
5	Male	−	−	−	+	−
6	Male	+	−	−	+	−

Note: −, no disease; +, obliteration of the intralabyrinthine fluid spaces; *, enhancement inside the membranous labyrinth.

[a] NA, not applicable.

TABLE 2: Frequency of obliteration of the different parts of the intralabyrinthine fluid spaces in six patients with Cogan syndrome (12 membranous labyrinths)

Part of the ML Involved	Number of MLs in Which Part Is Involved
Superior semicircular canal	8
Common crus	8
Lateral semicircular canal	7
Posterior semicircular canal	6
Basal turn of cochlea	5
Vestibule	4
Second turn of cochlea	2

and enhancement was seen inside these structures after gadolinium administration. In all patients the T2-weighted spin-echo images were normal and failed to demonstrate disease. The semicircular canals were more often involved than the vestibule and cochlea. The frequencies of obliteration of the lumen of these ML structures are listed in Table 2.

Discussion

Cogan described in 1945 for the first time a unique syndrome characterized by nonsyphilitic interstitial keratitis and vestibuloauditory dysfunction (1). Later, Cody and Williams (12) emphasized the systemic manifestations of this syndrome (12). The cause and pathogenesis are still unknown, but viral infection, autoimmune disease, and systemic (vascular) disease are mentioned in the etiology. Most often young adults are affected and symptoms usually develop during the second through fifth decades of life (1). Treatment consists of high-dose glucocorticoid therapy. Serious clinical outcomes, especially deafness, and less often vasculitis, aortic insufficiency, blindness, and even death have been reported.

The temporal-bone disease of Cogan syndrome has been described (2, 3, 13). Thickening of the membranous lining of the ML, hypertrophy of the stria vascularis, obliteration of the endolymphatic ducts of the cochlea and semicircular canals by an acidophilic coagulum, cellular debris inside the scala media and connective tissue in the scala tympani and scala vestibuli (3), and even new bone formation or osteogenesis (2, 13) have been reported. New bone formation should be visible on CT.

In the autopsy reports (2, 13), bone was found in the cochlea in the apical turns and near the round window niche and was also discovered in the semicircular canals. In our study new bone formation or calcification was present near the round window in cases 4 and 6 (Fig 2A) and bony narrowing of the lateral semicircular canal was seen in case 6. It was mentioned by Wolff et al (2) that connective tissue disease precedes formation of new bone. CT is unable to detect soft-tissue obliteration of the IFS, but MR has the potential to show soft-tissue obliteration because it better shows the fluid inside the lumen of the ML. Routine T1- and T2-weighted spin-echo images are 3 to 4 mm thick and therefore some parts of the ML and IFS are missed because of partial volume artifacts. In our study, soft-tissue obliteration of the IFS could not be detected on the T1- and T2-weighted spin-echo images. Partial voluming artifacts and the low signal intensity of the intralabyrinthine fluid, only slightly hyperintense compared with the surrounding bony labyrinth, can explain the poor performance of T1 images. It is harder to explain the lack of sensitivity of the T2-weighted images. Again, partial volume artifacts may be responsible but another possible explanation is that the thickening of the membranous lining and the hypertrophy of the stria vascularis of the ML have a signal intensity close to the signal intensity of the intralabyrinthine fluid and are consequently difficult to recognize.

3DFT gradient-echo techniques are better suited for the study of small structures like the labyrinth because they provide thin, 1-mm contiguous sections (4, 5, 14–16). Moreover, they display the intralabyrinthine fluid as high signal in contrast to the surrounding low signal of the bony labyrinth. In a study of 50 normal inner ears, high signal intensity inside the cochlea, vestibule, and semicircular canals was always seen on 3DFT CISS images (4). Recently, good results were also reported with 1-mm contiguous fast spin-echo images (17).

We found soft-tissue obliterations that were not seen on CT images in 5 of the 6 patients. In the two patients with calcifications inside the IFS on CT, more extensive soft-tissue obliterations were found in other parts of the IFS on the 3DFT CISS images (Fig 2B–C). This proves that soft-tissue obliteration is more frequent than bony obliteration and supports the hypothesis of Wolff et al (2) that abnormal connective tissue in the IFS probably precedes formation of new bone. These results also reveal better contrast between fluid and soft tissues inside the IFS on 3DFT CISS images than on T2-weighted spin-echo images.

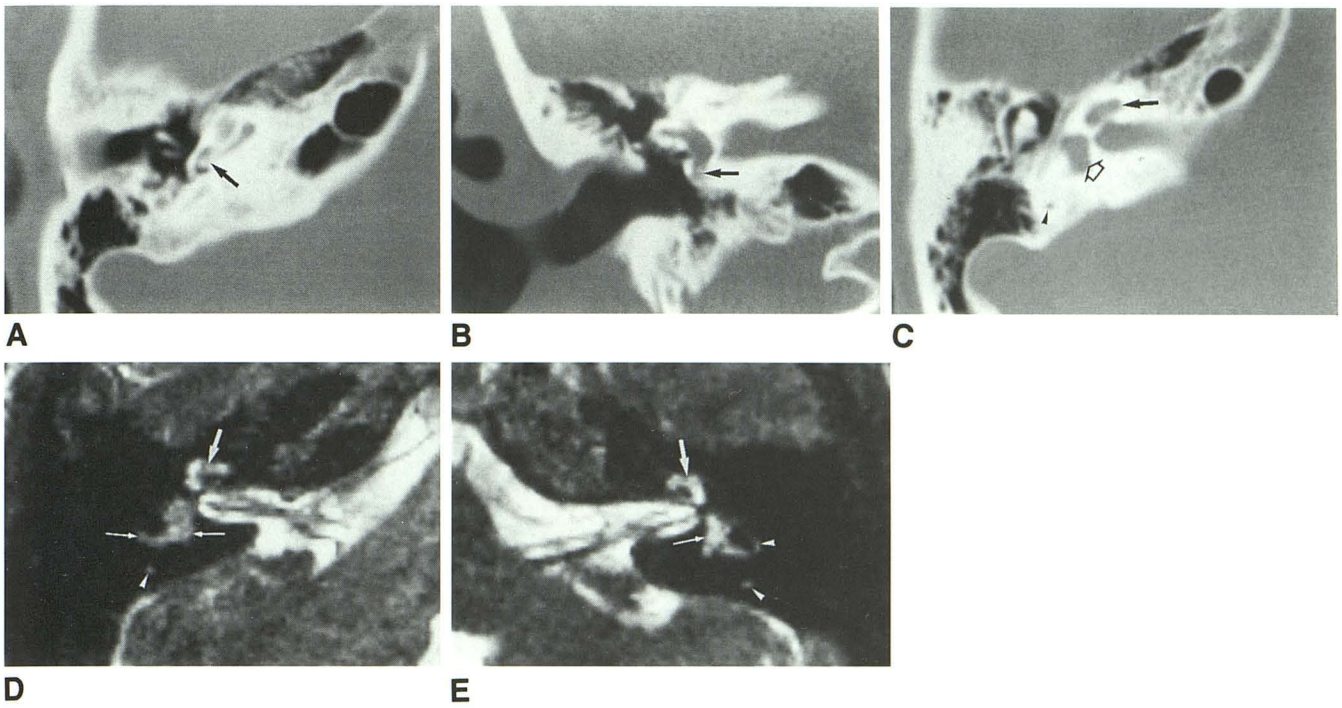

Fig. 2. Axial and coronal CT scan of the right temporal bone at the level of the basal turn of the cochlea (*A*, *B*) and axial CT (*C*) and 1-mm-thick three-dimensional CISS MR image (20/8/1) (*D*) at the level of the right vestibule and three-dimensional CISS MR image through the left vestibule (*E*) for comparison (case 6).

A, Calcification is present inside the basal turn of the cochlea near the round window niche (*arrow*).

B, On this coronal CT image the calcification can again be seen in the basal turn of the cochlea (*arrow*).

C, Normal low-density fluid is seen in the right cochlea (*large black arrow*), vestibule (*open black arrow*), and posterior semicircular canal (*black arrowhead*) on the CT image.

D, The corresponding CISS MR image demonstrates intermediate signal intensity in the posterior semicircular canal (*white arrowhead*), vestibule and lateral semicircular canal (*long white arrows*), and in the anterior part of the cochlea (*large white arrow*). Normally the signal intensity of the fluid inside these structures is isointense with the cerebrospinal fluid inside the internal auditory canal but in this patient the high signal of the intralabyrinthine fluid is replaced by soft tissue. Fluid can be recognized only in parts of the cochlea and around the cochlear and inferior vestibular nerve inside the internal auditory canal.

E, This CISS image through the left labyrinth shows that normal high-signal fluid is visible in the anterior part of the cochlea (*large white arrow*), vestibule (*thin white arrow*), and in the visible parts of the lateral and posterior semicircular canals (*white arrowheads*). The signal in these structures is isointense with the signal of cerebrospinal fluid in the internal auditory canal.

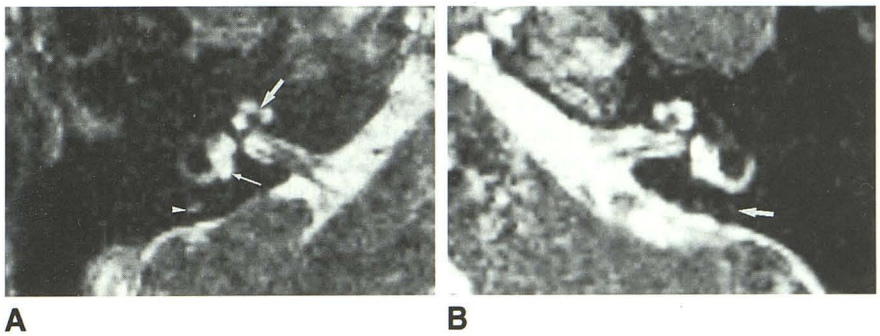

Fig. 3. Axial three-dimensional CISS MR image (20/8/1) through the right (*A*) and left (*B*) labyrinth at the level of the lateral semicircular canal (case 5).

A, Normal high-signal-intensity fluid, isointense with the fluid in the internal auditory canal and cerebellopontine angle, can be seen inside the cochlea (*large white arrow*), vestibule (*thin white arrow*) and posterior semicircular canal (*white arrowhead*). The 3DFT CISS images of 50 normal inner ears proved that high signal intensity inside the cochlea, vestibule, and the three semicircular canals is always visible (4).

B, On the left side the high signal intensity of the fluid inside the posterior semicircular canal is absent (*arrow*), representing "bony" or "soft tissue" obliteration. However the corresponding CT image showed a normal patent posterior semicircular canal, proving that the obliteration seen on the MR image was caused by soft tissues.

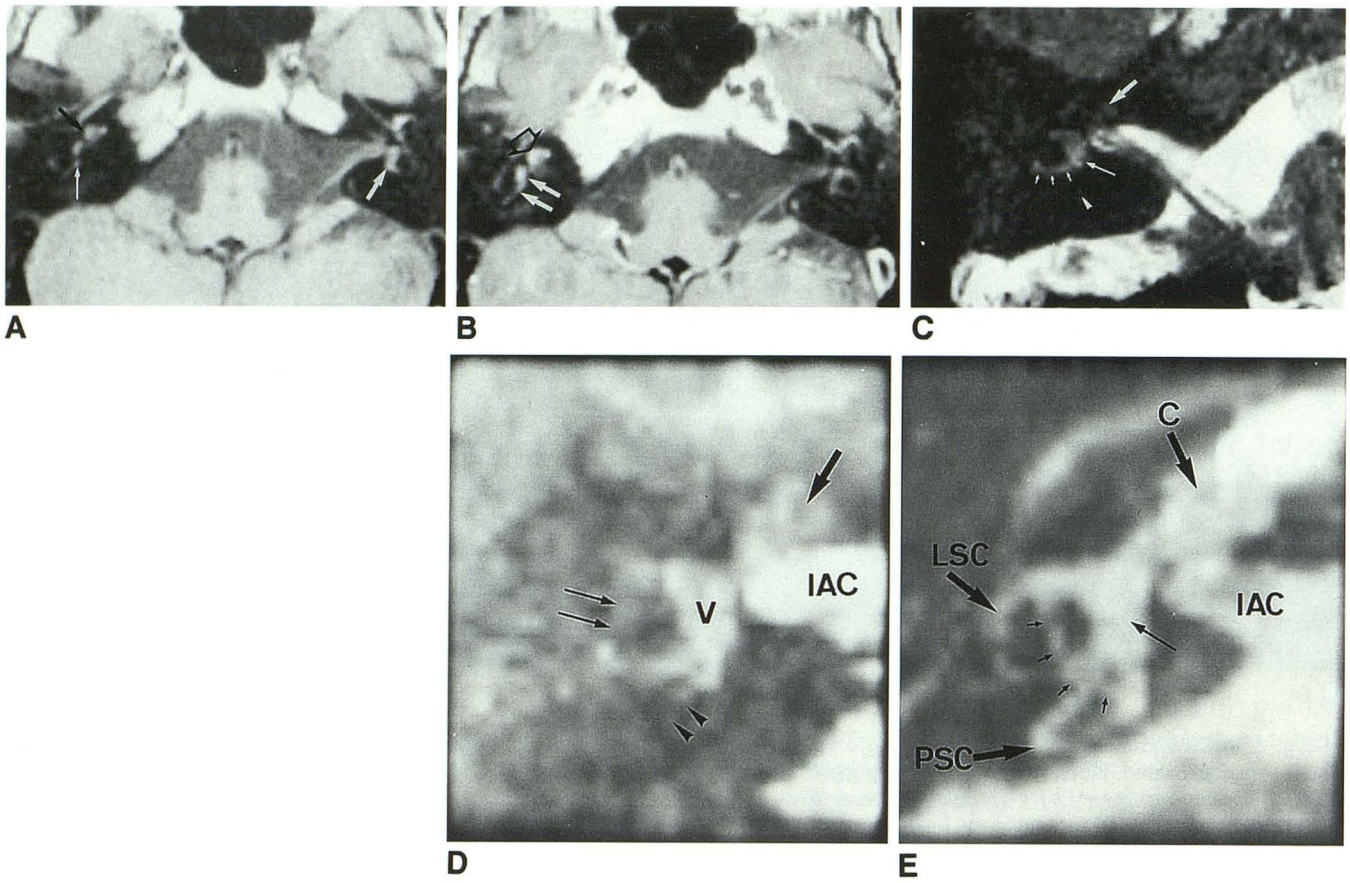

Fig. 4. Axial 3-mm-thick unenhanced (*A*) and gadolinium-enhanced (*B*) T1-weighted images (500/15/4) through both labyrinths; axial three-dimensional CISS MR image (20/8/1) through the right labyrinth (*C*); three-dimensional reconstructions of the right labyrinth (*D*) (case 2); and normal three-dimensional labyrinth reconstruction (*E*) for comparison.

A, High signal intensity is seen in the right cochlea (*black arrow*), right posterior semicircular canal (*thin white arrow*), and left vestibule (*large white arrow*). Normally on T1-weighted images intralabyrinthine fluid is isointense with the cerebrospinal fluid in the internal auditory canal and cerebellopontine angle.

B, Enhancement is seen inside the cochlea (*open black arrow*) and vestibule and posterior semicircular canal (*white arrows*) after intravenous gadolinium administration.

C, The high signal intensity of fluid is lost completely in the cochlea (*large white arrow*), vestibule (*thin white arrow*), and lateral semicircular canal (*small white arrows*) and is replaced by "soft tissue" intermediate signal intensity. The posterior semicircular canal is completely obliterated and all signal inside the canal is lost (*white arrowhead*).

D, The three-dimensional reconstruction of the right labyrinth confirms loss of high-signal-intensity intralabyrinthine fluid in the total cochlea (*large black arrow*), posterior semicircular canal (*black arrowheads*), and in the lateral semicircular canal (*thin black arrows*). Even in the vestibule (V) signal loss is recognized (compare with the high signal intensity in the internal auditory canal). The superior semicircular canal is completely obliterated and can not be seen. On the axial 1-mm-thick CISS image (*C*) the anterior part of the lateral semicircular canal is missing, but this could have been because of an oblique cut through the canal. However on the three-dimensional reconstructions the anterior part of the canal is still absent proving that the signal loss is caused by obliteration of the canal and not by an oblique cut through the canal.

E, The fluid-filled lateral semicircular canal (LSC), posterior semicircular canal (PSC), superior semicircular canal (*small black arrows*), the cochlea (*C*), and the vestibule (*thin black arrow*) can all be seen as high signal intensity structures on a three-dimensional reconstruction of a normal labyrinth. *IAC* designates the internal auditory canal.

In one patient no obliterations were found on CT nor on the most sensitive (3DFT CISS) MR images. This was also the only patient with a complete recovery of the sensorineural hearing loss, suggesting that patients with a less severe clinical presentation have less chance of obliteration of the IFS. In the other five patients, narrowing or obliteration of parts of the semicircular canals (Figs 2, 3) was seen on the 3DFT images; in three of these patients abnormal soft tissues were also found in the vestibule (Figs 2, 4). This correlated well with the clinical findings. All five patients suffered from vertigo. In three patients (cases 2, 4, and 6), parts of the cochlea were obliterated (Figs 2, 4) and again these findings were consistent with the audiometry. In two patients, however (cases 3 and 5), deafness or subtotal deafness was found clinically but normal

cochlear structures were seen on MR and CT. This shows that the radiologic-clinical correlation is good but not perfect.

In only one patient was high signal intensity seen inside the cochlea, vestibule, and semicircular canals on the unenhanced T1-weighted images, and enhancement was seen in these structures on the right side after gadolinium administration (Fig 4). The patient was completely deaf on both sides and showed no response to caloric stimuli at the time of CT and MR examination. High signal inside the ML on unenhanced T1-weighted images has been described in two patients with sudden hearing loss and vertigo (18). Fast or slow flow are unlikely causes for the hyperintensity on the unenhanced images but high protein content inside the intralabyrinthine fluid cannot be excluded as possible explanation (18). However, the association of Cogan syndrome and systemic vascular disease is known and lesions resembling those seen in polyarteritis nodosa and thromboangiitis obliterans were found in patients with Cogan syndrome (3). Moreover, hemorrhage into the IFS was seen in animals after experimental venous occlusion (19). Therefore, hemorrhage seems to be the most likely explanation for the high signal intensity inside the perilymphatic and endolymphatic spaces on unenhanced T1-weighted images.

Gadolinium enhancement in the ML has also been studied (5, 20, 21) and represents gadolinium leakage through the abnormal labyrinth membrane. This has been reported in cases of viral, luetic, and bacterial labyrinthitis (20, 21) and in cases of intralabyrinthine schwannoma (5, 22).

Ischemia or vasculitis are also mentioned as a possible cause. The ML has precarious vascularization and no collateral circulation (23). As already mentioned, vasculitis is frequently found in patients with Cogan syndrome (1, 3). Moreover, Perlman et al (13) observed osteogenesis and diseased soft tissues in the inner ear after experimental obstruction of the arterial supply of the inner ear in guinea pigs (24). These findings suggest that the enhancement seen in our patient is most likely caused by vasculitis and probably represents active disease.

Conclusions

1) In the majority of patients with Cogan syndrome, obliterations of the intralabyrinthine fluid spaces are found on CT or MR.

2) CT is the most sensitive technique to detect bony obliteration. 3DFT CISS MR imaging is the most sensitive technique to detect the far more frequent soft-tissue obliteration.

3) Hyperintensity inside the ML on precontrast T1-weighted images (seen in one patient) probably represents hemorrhage. Gadolinium enhancement of the ML in patients with Cogan syndrome represents gadolinium leakage through an abnormal labyrinthine membrane and probably represents active disease.

References

1. Vollertsen RS, McDonald TJ, Younge BR, Banks PM, Stanson AW, Ilstrup DM. Cogan's syndrome: 18 cases and a review of the literature. *Mayo Clin Proc* 1986;61:344–361
2. Wolff D, Bernhard WG, Tsutsumi S, Ross IS, Nussbaum HE. The pathology of Cogan's syndrome causing profound deafness. *Ann Otol Rhinol Laryngol* 1965;74:507–520
3. Fisher ER, Hellstrom HR. Cogan's syndrome and systemic vascular disease: analysis of pathologic features with reference to its relationship to thromboangiitis obliterans (Buerger). *Arch Pathol* 1961;72:572–592
4. Casselman JW, Kuhweide R, Deimling M, Ampe W, Dehaene I, Meeus L. Constructive interference in steady state (CISS)-3DFT MR imaging of the inner ear and cerebellopontine angle. *AJNR Am J Neuroradiol* 1993;14:47–57
5. Casselman JW, Kuhweide R, Ampe W, Meeus L, Steyaert L. Pathology of the membranous labyrinth: Comparison of T1-, and T2-weighted and gadolinium-enhanced spin-echo and 3DFT-CISS imaging. *AJNR Am J Neuroradiol* 1993;14:59–69
6. Cogan DG. Syndrome of nonsyphilitic interstitial keratitis and vestibuloauditory symptoms. *Arch Ophthalmol* 1945;33:144–149
7. Patz S. Some factors that influence the steady state in "steady state" free precession. *Magn Reson Imaging* 1988;6:405–413
8. Deimling M, Laub GA. Constructive interference in steady state for motion sensitivity reduction (abstr). In: *Book of abstracts: Society of Magnetic Resonance in Medicine 1989*, Vol. 1. Berkeley, CA: Society of Magnetic Resonance in Medicine, 1989:842
9. Gyngel ML, Palmer ND, Eastwood LM. The application of steady state free precession (SSFP) in 2DFT MR imaging (abstr). In: *Book of abstracts*, Vol. 3. Berkeley, CA: Society of Magnetic Resonance in Medicine, 1986:666
10. Oppelt A, Graumann R, Barfuss H, Fischer H, Hartl W, Schajor W. FISP, a new fast MRI sequence. *Electromedica* 1986;54:15–18
11. Laub GA, Kaiser WA. MR angiography with gradient motion refocusing. *J Comput Assist Tomogr* 1988;12:377–382
12. Cody DTR, Williams HL. Cogan's syndrome. *Laryngoscope* 1960;70:447–478
13. Rarey KE, Bicknell JM, Davis LE. Intralabyrinthine osteogenesis in Cogan's syndrome. *Am J Otolaryngol* 1986;4:387–390
14. Tanioka H, Shirakawa T, Machida T, Sasaki Y. Three dimensional reconstructed MR imaging of the inner ear. *Radiology* 1991;178:141–144
15. Brogan M, Chakeres DW, Schmalbrock P. High-resolution 3DFT MR imaging of the endolymphatic duct and soft tissues of the otic capsule. *AJNR Am J Neuroradiol* 1991;12:1–11
16. Tanioka H, Machida T, Zusho H. High resolution MRI of the temporal bone using a surface coil: normal anatomy. *Jpn J Med Imaging* 1989;8:2–8

17. Tien RD, Felsberg GJ, Macfall J. Fast spin-echo high-resolution MR imaging of the inner ear. *AJR Am J Roentgenol* 1992;159:395–398
18. Weissman JL, Curtin HD, Hirsch BE, Hirsch WL. High signal from the otic labyrinth on unenhanced magnetic resonance imaging. *AJNR Am J Neuroradiol* 1992;13:1183–1187
19. Perlman H, Kimura R. Experimental obstruction of venous drainage and arterial supply of the inner ear. *Ann Otol Rhinol Laryngol* 1957;66:537–546
20. Seltzer S, Mark AS. Contrast enhancement of the labyrinth on MR scans in patients with sudden hearing loss and vertigo: evidence of labyrinthine disease. *AJNR Am J Neuroradiol* 1991;12:13–16
21. Mark AS, Seltzer S, Nelson-Drake J, Chapman JC, Fitzgerald DC, Gulya AJ. Labyrinthine enhancement on gadolinium-enhanced magnetic resonance imaging in sudden deafness and vertigo: correlation with audiologic and electronystagmographic studies. *Ann Otol Rhinol Laryngol* 1992;101:459–464
22. Brogan M, Chakeres DW. Gd-DTPA-enhanced MR imaging of cochlear schwannoma. *AJNR Am J Neuroradiol* 1990;11:407–408
23. Schuknecht HF. *Pathology of the ear.* Cambridge, MA: Harvard University, 1974;61:258–262
24. Perlman H, Kimura R, Fernandez C. Experiments on temporary obstruction of the internal auditory artery. *Laryngoscope* 1959;69:591–613